DRYING TECHNOLOGY, 19(2), 281–296 (2001)

# STRUCTURAL MODELS RELATED TO TRANSPORT PROPERTIES FOR THE DRIED LAYER OF FOOD MATERIALS UNDERGOING FREEZE-DRYING

**Yasuyuki Sagara**

Department of Global Agricultural Sciences,
Graduate School of Agricultural and Life Sciences,
The University of Tokyo,
1-1-1, Yayoi, Bunkyo-ku, Tokyo, 113-8657, Japan

## ABSTRACT

The values of thermal conductivity and permeability have been presented for the dried layer of raw beef, coffee solutions and sliced as well as mashed apples. A structural model for beef, coffee solution and mashed apple was developed for predicting the permeability of water-vapor flowing through the dried layer. In modeling the porous dried layer was assumed to be a bundle of capillary tubes with the pore space having an equivalent pore radius, porosity, and tortuosity factor. These results indicated that the structure for the solution systems was controllable by both solute concentration and freezing manners.

Another cellular structural model has been presented for predicting the permeability of a sliced apple. The resistance of a cell membrane to the molecular transfer of water vapor was determined from the value of permeability and the size as well as number of the cells existed in the dried layer. Since the drying rate of cellular materials was limited by the mass flux across the dried layer, the model was considered to play an important role in predicting the optimum heating program for the surface temperature of cellular food materials such as fresh fruits and vegetables.

*Key Words:* Apple; Beef; Coffee; Freezing rate; Pore radius; Porosity; Permeability; Structural model; Thermal conductivity.

## INTRODUCTION

Freeze-drying has had a great impact upon the production of dehydrated foods because of the superior quality of the product obtained and promises continued expansion of the number of applications. However, the process is only feasible if the cost of production can be lowered by optimum plant operations. Since the freeze-drying rate is limited by the rates of heat and mass transfer across a dried layer, the values of its thermal conductivity and permeability are indispensable to determine the drying rate. These values are mainly governed by the structure of the dried layer and the operating factors such as temperature and pressure. Since the structural nature of the dried layer is also affected by freezing operations, the relationships among the freezing condition, structure and transport properties of the dried layer are the fundamental information to design the optimum drying cycle and control the quality of final products.

This paper presents (1) the values of thermal conductivity and permeability for the dried layer of several food materials, (2) the structural models for predicting the value of permeability, and then (3) demonstrates the effects of freezing rate, operating temperature as well as pressure on the values of transport properties.

## THEORETICAL MODEL

### Model for Transport Properties Analysis

FIGURE 1 shows a uniformly-retreating-ice front (URIF) model to determine the transport properties for the dried layer of the material undergoing freeze-drying. Based on several assumptions, the equations of heat and mass flux were introduced to the dried layer for obtaining the equations to determine the values of thermal conductivity and permeability from drying data (Sagara & Hosokawa, 1982).

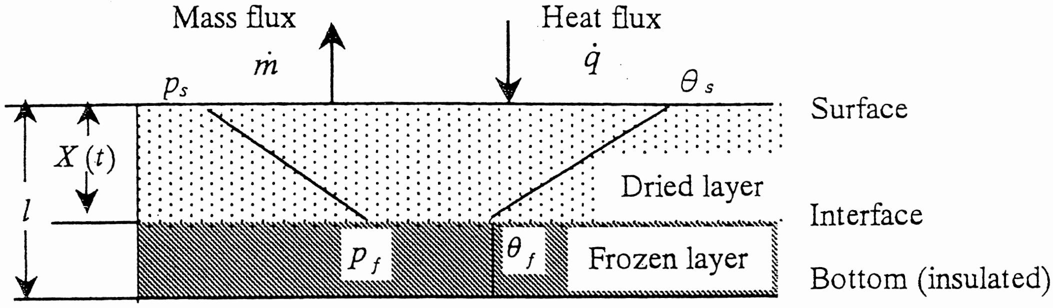


*Figure 1.* Freeze-drying model to determine transport properties.

## Structural Model

1) Capillary Model

An approximate method was developed for predicting the structural parameters of the dried layer by assuming this layer to be a bundle of capillary tubes with the pore space having an equivalent pore radius, porosity and tortuosity factor. The mass flux density of water vapor flowing through the dried layer may be written as:

$$\dot{m} = -\frac{KM_w}{RT} \, grad \; p \tag{1}$$

The expressions for the permeability coefficient of a single capillary tube are taken from Mellor and Lovett (1964);

$$K = \frac{\varepsilon}{\tau} D_k \Omega \tag{2}$$

where,

$$\Omega = \underset{\text{(Poiseulle)}}{\frac{3\pi}{64}\frac{r}{\lambda}} + \underset{\text{(Slip)}}{\frac{\pi}{4}\frac{2r/\lambda}{(1+2r/\lambda)}} + \underset{\text{(Knudsen)}}{\frac{1}{1+2r/\lambda}} \tag{3}$$

In this equation the value of $\Omega$ expresses the total of separate contributions due to Poiseulle's flow, slip flow and Knudsen's flow. From the above relation, $\Omega$ can be expressed as a function of $r$ and $T/p$ since $\lambda$ is defined in term of a ratio of absolute temperature to pressure. The mean free path of a water-vapor molecule $\lambda$ is given by

$$\lambda = \frac{\kappa T}{\sqrt{2}\pi\sigma_w^2 P} \tag{4}$$

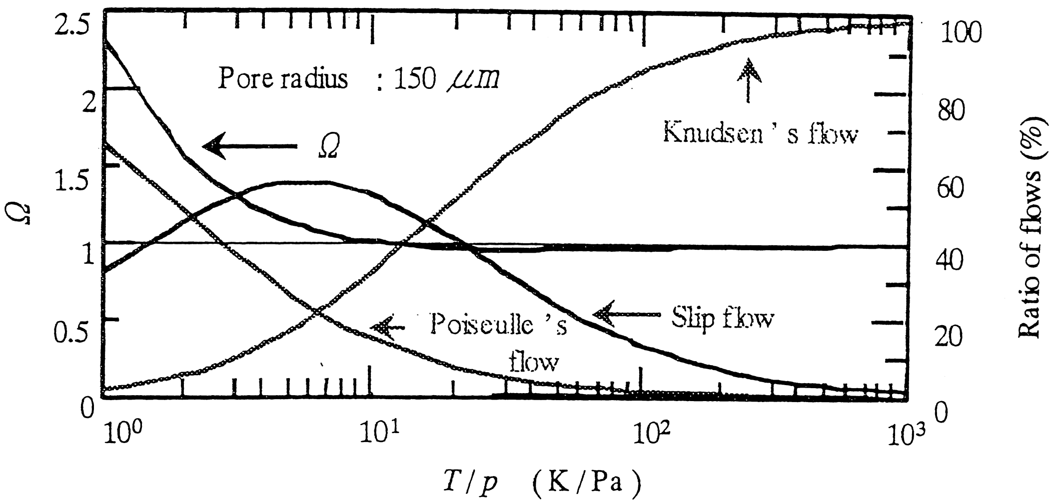


*Figure 2.* Variation of $\Omega$ with $T/p$ and the ratios of flows contribute to $\Omega$.

The Knudsen diffusivity was defined in terms of the pore radius and the average molecular velocity as follows:

$$D_k = \frac{2}{3}\bar{v}r, \quad \text{where} \quad \bar{v} = \left(\frac{8RT}{\pi M_w}\right)^{1/2} \tag{5}$$

Since the pore radius of several freeze-dried foods is in the range of 10-300 μm, the effects of $T/p$ as well as each flow on $\Omega$ were investigated and then illustrated as shown in FIGURE 2, assuming the equivalent pore radius of 150 μm. The curve of $\Omega$ has been found to approach unity with an increase in the ratio of Knudsen's flow to the total. Since in usual operating conditions the ratio $T/p$ is assessed to be in the range of 4 to 10, the function $\Omega$ can be approximated to be unity. Then the pore structural ratio $r/\tau$ is estimated from equations (2) and (5). Combining these equations, one get

$$K = A\sqrt{T}, \quad \textit{where} \quad A = \frac{r}{\tau}\varepsilon\frac{2}{3}\left(\frac{8R}{\pi M_w}\right)^{1/2} \tag{6}$$

As indicated in equation (6) the slope of a curve fitted to the plot of permeability against $\sqrt{T}$ provide the constant value $A$ and thus the ratio $r/\tau$ can be determined.

After obtaining the values of structural parameter, they were applied to an equation presented by Mellor & Lovett (1964), which was derived on the basis of collision theory for the permeability in term of the mean free path, giving

$$K = \frac{\varepsilon}{\tau} D_k \left[ \left\{ \frac{3}{32k'} \frac{2r}{\lambda} + \delta_1 \right\} \cdot (1 - e^{-2r/\lambda}) + e^{-2r/\lambda} \right] \tag{7}$$

As shown in the following section the equation (7) has been found to fit the experimental results for raw beef and coffee solutions over the wide pressure ranges.

2) Cellular Structural Model

Values of the permeability for sliced apples calculated by the capillary model were found to be more than 10 times greater than those of measured. As an alternative a cellular structural model has been proposed as shown in FIGURE 3. In the model, a cell is assumed to be a cylindrical geometry having an equivalent diameter $d_c$ and $l_c$ in length, respectively. The $n$ layers of the cell are stacked parallel to the direction of water vapor transfer within the distance $X(t)$ between the surface and sublimation front of the sample. By utilizing the analogy of electrical circuit, the resistance against the water vapor $R_n$ was determined as the summation of an equivalent resistance $R_s$ of each membrane. These two structural parameters were then introduced to modify the equation (2) for single capillary tube as follows;

$$K = \left(\frac{\varepsilon}{\tau} D_k \Omega\right) / R_n \tag{8}$$

$$R_n = (n+1)R_s; R_0 = 1 \tag{9}$$

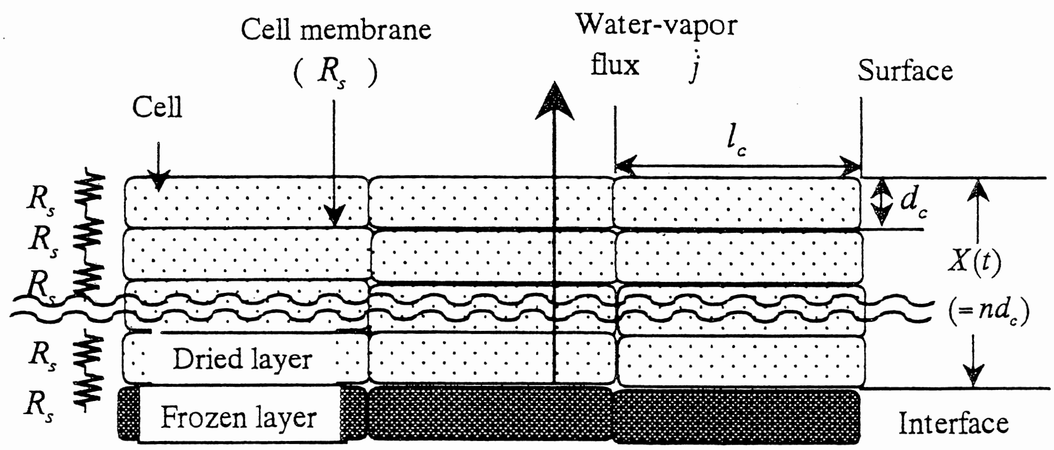


*Figure 3.* Structural model for cellular food materials.

In the modified model the tortuosity factor $\tau$ was assummed to be unity because of the assumption of cells connected in series, and also the value of $\Omega$ can be assumed to be unity under our experimental conditions.

As above-mentioned, the parameter $R_s$ can be calculated by carrying out once-time freeze-drying experiment and the microscopic observation of average diameter of cells, and thus the value of permeability could be determined for sliced samples. However, the availability of the model depends on some factors such as the average diameter of cells, accuracy of temperature measurement as well as control at the sample surface and geometrical stability of sublimation front that is foreseen to be lost by thermal edge effect during the later period of sublimation dehydration. To avoid these problems the average diameter of cells should be measured in the direction of mass or water-vapor transport, and the model is recommended to be applied during the period until the sublimation front reaches about 60% of sample thickness.

The proposed model can be applied to other cellular food materials, and a predicted value is useful to calculate the mass transfer rate across the dried layer, and finally, it can be used to design optimum plant operations, or heating program for the surface of material whose drying rate is limited by mass transfer rate.

## RESULTS AND DISCUSSION

### Transport Properties

1) Raw Beef

The relationship between thermal conductivity and the pressure of the dried layer is shown in FIGURE 4. Thermal conductivity $\lambda^*$ plotted in this figure is determined by neglecting the heat absorbed by water vapor flowing through the dried layer. Using a steady state method, Harper (1962) and Harper & El Sahrigi (1964) measured the thermal conductivity on freeze-dried beef, peach, apple and other materials with air or other high-conductivity gases surrounding the sample over a pressure range of 0.67 Pa to atmospheric. They concluded that the experimental data could be adequately correlated by an empirical equation based on concepts of unit cells involving combinations of series and parallel arrangements of the individual solid and gas phases. Since no data are given for beef in the presence of water vapor, a curve in FIGURE 4 was calculated by applying the recommended values for air-filled beef to the empirical equation. However, there is some indication that the empirical equation does not accurately describe the thermal conductivity of freeze-dried beef when the

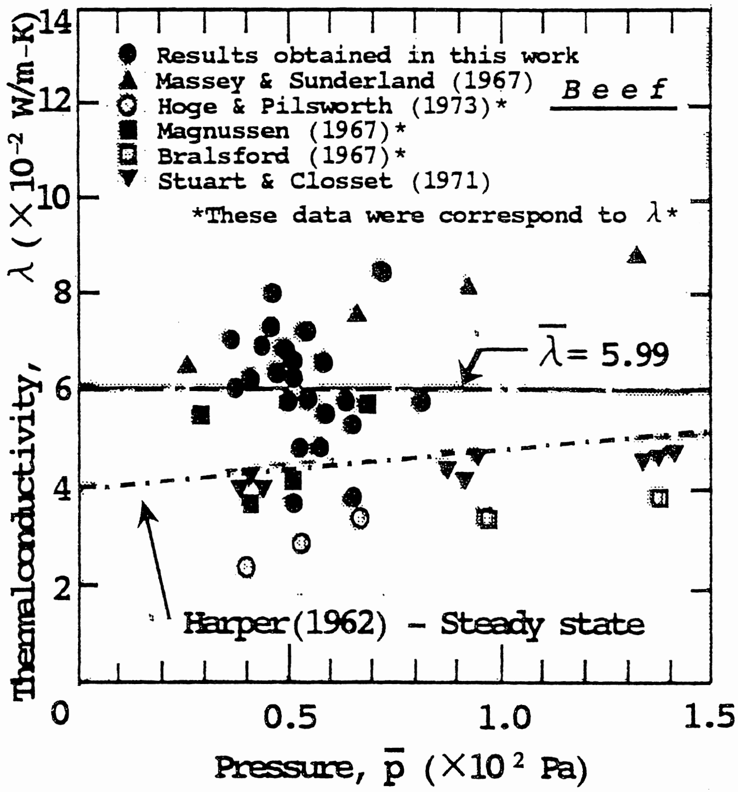


*Figure 4.* Thermal conductivity vs. pressure for raw beef.

surrounding gas is water vapor. Bralsford (1967) and Hoge & Pilsworth (1973) indicated that their results for freeze-dried beef surrounded by water vapor were significantly different from those obtained with non-condensing gases and the values lay increasingly far above those for air. Triebes & King (1966) also reported the same behavior for freeze-dried cooked turkey meat. Our own data were found to be greater than would be predicted for air-filled beef and appeared to confirm in this respect.

Although the effect of pressure on thermal conductivity was not recognized in our pressure range, it was considered that the conductivity essentially had a tendency to increase as the pressure increase. It is well known that the thermal conductivities of porous materials, when plotted vs. the logarithm of the pressure of the surrounding gas, provides characteristic sigmoid curves, indicating both lower and higher constant values in the low-pressure region below about 10 Pa and high-pressure above about 15 kPa, respectively. The lower constant value corresponds to the intrinsic conductivity of the solid and the higher to the apparent thermal conductivity of gas-filled solid matrix. The data plotted in FIGURE 4 all fell in

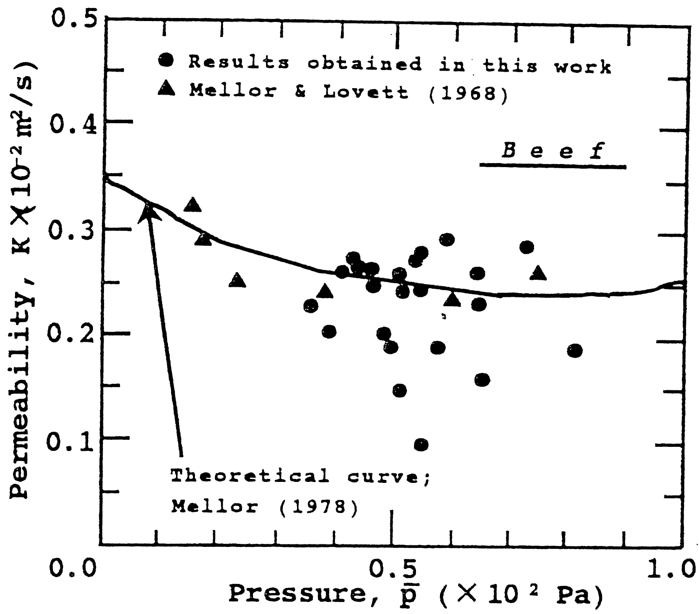


*Figure 5.* Permeability vs. pressure for raw beef.

intermediate pressure region in which $\lambda$ should increase with an increase in pressure. As shown in these results the contribution of gas phase confined in a solid matrix to the heat conduction process should be dependent upon the pressure level. The kinetic theory predicts that the gas thermal conductivity is independent of pressure as long as the mean free path is small compared with the sizes of void space in the matrix; as a consequence, the apparent thermal conductivity of the gas-filled solid matrix is independent of pressure. As the pressure is reduced, with the mean free path becoming comparable to and greater than the pore spacing, the gas thermal conductivity and thus the apparent conductivity of the matrix should begin to decrease continuously. At very low pressures, the gas provides a negative contribution to the total heat conduction, and thus a lower asymptotic conductivity of the solid matrix should be reached.

Plots of permeabilities vs. pressure are shown in FIGURE 5. The values of $K$ were in good agreement with Mellor's theoretical curve based on a collision theory and also with their experimental data using completely freeze-dried samples under steady-state conditions. TABLE 1 shows the numerical values of the constant applied to the equation (7). As discussed by Mellor (1978), the theoretical curve demonstrated that the flow condition of water vapor transformed from Knudsen's flow to slip flow as the pressure increased.

*Table 1.* Numerical Values of the Constant Used to Calculate the Permeability of Beef Sample by Equation (7)

| Constants | Numerical value used | Origin |
|---|---|---|
| r | $58 \times 10^{-6}$, m | Mellor (1978) |
| $k'$ | 2.5, - | Mellor and Lovett (1964) |
| $\tau$ | 4.2, - | Mellor (1978) |
| $\delta_1$ | $3\pi/16$, - | Mellor and Lovett (1964) |
| $\sigma$ | $4.6 \times 10^{-10}$, m | Kennard (1938) |
| $\varepsilon$ | 0.64, - | Harper (1962) |

2) Coffee Solution

FIGURE 6 shows the relationship between thermal conductivity and the porosity of the dried layer for coffee solutions. The result showed clearly that the thermal conductivity was markedly affected by solute concentration or the porosity of the dried layer. Porosity was assessed from

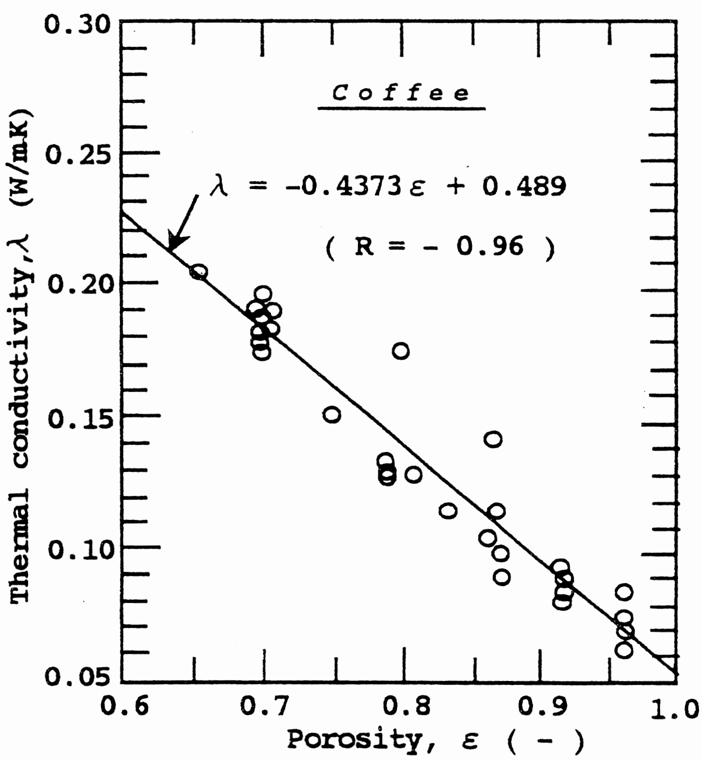


*Figure 6.* Thermal conductivity vs. porosity for coffee solutions.

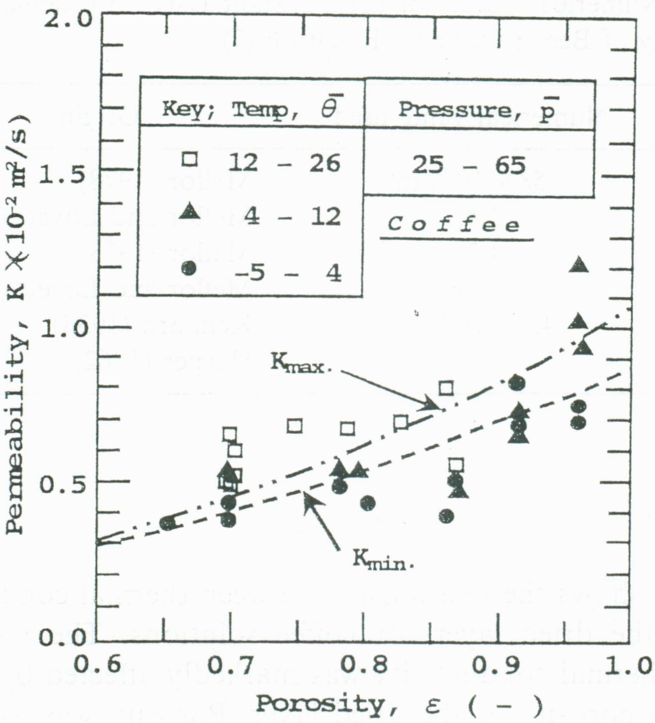


*Figure 7.* Permeability vs. porosity for coffee solutions.

cumulative composition using the value of 0.625 for the specific volume of pure coffee soluble. A linear relationship between thermal conductivity and porosity was obtained and the equation for a regression line fitted to all of the data is also presented in FIGURE 6.

FIGURE 7 shows the relationship between permeability and porosity for coffee solutions at various temperatures of the dried layer. The permeability was found to depend mainly on the solute concentration or porosity of the dried layer and then other operating factors such as temperature or pressure. For example, the permeabilities for all samples of 40% in concentration ($\varepsilon = 0.7$) were found to increase with an increase in the temperature of the dried layer. As is obvious from the kinetic theory of an ideal gas, the mean translational kinetic energy of a gas molecule is proportional to the absolute temperature. In accordance with this interpretation the heat transfer from solid matrix to the molecules of water vapor is considered to accelerate their flow rate, providing the greater value of permeability. However, no theoretical investigation has been presented on heat transfer by both intermolecular and wall collisions for condensable gas such as water vapor. Although the pressure dependence of permeability was not definitely recognized in our pressure range, it has been demonstrated that the permeability increases as the pressure increase as indicated by freeze-dried beef

*Table 2.* Variation of Pore Radius with Porosity for the Dried Layer of Coffee Solutions

| Pore radius | Porosity | | | | |
|---|---|---|---|---|---|
| | 0.7 | 0.8 | 0.86 | 0.92 | 0.96 |
| r; Eq. (2) | 59.4 | 70 | 70.9 | 95.4 | 117.5 |
| r′; Eq. (8) | 76.5 | 88.1 | 89.6 | 122.4 | 149.9 |
| Δr; (%) | 28.8 | 25.9 | 26.3 | 28.3 | 27.6 |

samples. These behaviors were in good agreement with theoretical investigations based on the collision theory (Sagara, 1986) and also with experimental results obtained for concentrated tomato and sugar cane juices (Mellor, 1978).

As shown in TABLE 2 the equivalent pore radius *r* was predicted from the capillary model in the concentration range from 6.2 to 40.4%. The curve of $K_{max}$ in FIGURE 7 was calculated from the maximum values of temperature (26°C) as well as pressure (65 Pa), applying structural parameters obtained from equation (7). The calculation method of $K_{min}$ follows the same procedure (-5°C, 25 Pa) as for $K_{max}$. As these curves demonstrate a similar porosity-dependent behavior of experimental plots, the assumptions made in this model appeared to be essentially reasonable.

3) Apple

TABLE 3 shows the values of the thermal conductivity and permeability for several food materials obtained by the URIF model. In this TABLE the values of thermal conductivity for sliced and mashed apples were also presented. These data can be adequately calculated by the empirical equation presented by Harper (1962), and the thermal conductivity essentially had a tendency to increase as the pressure increased as indicated by raw beef samples. However, these absolute values were relatively larger than the empirical curve because in this study the "effective" value of thermal conductivity were measured under the existing conditions of temperature and pressure gradients across the dried layer of the sample undergoing freeze-drying.

Both resistance values of $R_n$ and $R_s$ in the cellular structural model were calculated for sliced apples by using measured values of permeability. The values of $R_n$ were in the range of 42.5 to 96.2, while those of $R_s$ were 2.9

*Table 3.* Thermal Conductivity and Permeability for Several Food Materials

| Material | Sample surface temperature (°C) $\theta_s$ | Pressure in the chamber (Pa) $p_s$ | Temperature* (°C) $\bar{\theta}$ | Pressure* (Pa) $\bar{p}$ | Thermal conductivity (W/m·K) $\lambda$ | Permeability ($\times 10^{-2} m^2/s$) K | Reference |
|---|---|---|---|---|---|---|---|
| Sliced apple | -10~10 | 20~30 | -17.7~-3.4 | 38.4~80.0 | 0.056~0.123 | 0.063~0.120 | Araki and Sagara et al. (1998) |
| Mashed apple (A)** | 0~40 | 20~30 | -13.6~8.5 | 33.5~46.2 | 0.11~0.13 | 0.40~0.50 | Araki and Sagara et al. (1998) |
| Mashed apple (B)** | 10~70 | 20~30 | -11.8~19.7 | 23.7~29.0 | 0.068~0.073 | 1.3~1.6 | Araki and Sagara et al. (1998) |
| Beef | 30~100 | 7~30 | 3.0~40.8 | 38.2~78.5 | 0.036~0.084 | 0.090~0.405 | Sagara et al. (1982) |
| Minced beef | 40 | 2.7~13.3 | 7.3~10.3 | - | 0.050~0.069 | 0.13~0.24 | Widodo and Tambunan (1996) |
| Coffee solution (6~30%)*** | 20~53 | 10~95 | -5.3~14.8 | - | 0.062~0.172 | 0.340~1.220 | Sagara and Hosokawa (1982) |
| Coffee solution (29~45%)*** | -7~71 | 7~12 | -14.1~26.1 | 47.1~66.8 | 0.153~0.277 | 0.213~0.649 | Sagara and Ichiba (1994) |
| Coffee solution (10~36%)*** | 60 | 22~34 | 12.9~20.2 | 24.9~64.9 | 0.063~0.144 | 0.508~4.235 | Ichiba (1994) |
| Shrimp | 30~50 | 7~133 | 4.2~21.2 | 53.6~263 | 0.038~0.086 | 0.031~0.120 | Wenur (1997) |

*Average value for the dried layer
**(A) Rapid freezing and (B) Slow Freezing
***Coffee solute concentration

to 7.3, and the average for them were determined to be 71.4 and 4.41, respectively. The mean values obtained for a sliced apple were used to predict the intrinsic permeability of apple flesh, and the predicted value was recognized to agree well with all measured permeability data under various drying conditions.

### Effect of Freezing Rate on Transport Properties

FIGURE 8 shows the freezing curves for mashed apple samples. The changes in temperature at the center during freezing could be regarded as an index of the freezing rate. Based on these indexes the mashed samples were classified into the groups A and B. The freezing rate of the group A was relatively larger than the group B. In order to obtain the quantitative index, the period between two inflection points was defined as the ice-crystallization time, based on the primary differential values of these curves.

FIGURE 9 shows a linear relationship between permeability and ice-crystallization time for mashed samples. This behavior is attributed to the larger ice crystals formed in the sample as the freezing rate decreased. Hence, the effects of the freezing rate on transport properties, especially on the permeability, were found to be critical for the mashed cellular food materials. In liquid food systems the porosity of the dried layer is governed by the solid content or concentration, and thus the porosity mainly affects

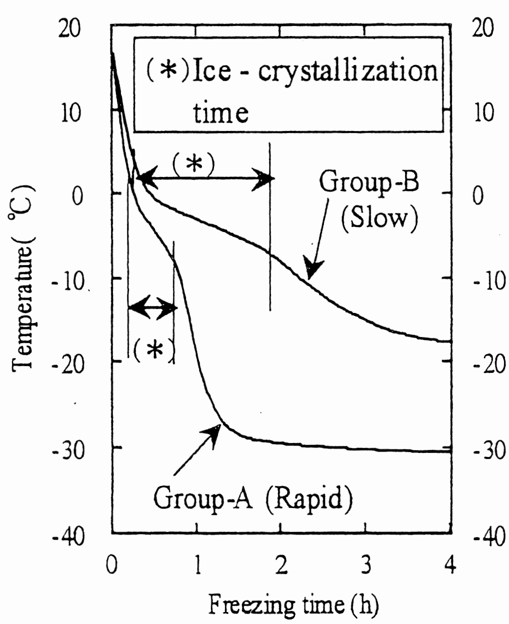


*Figure 8.* Freezing curve for mashed apples.

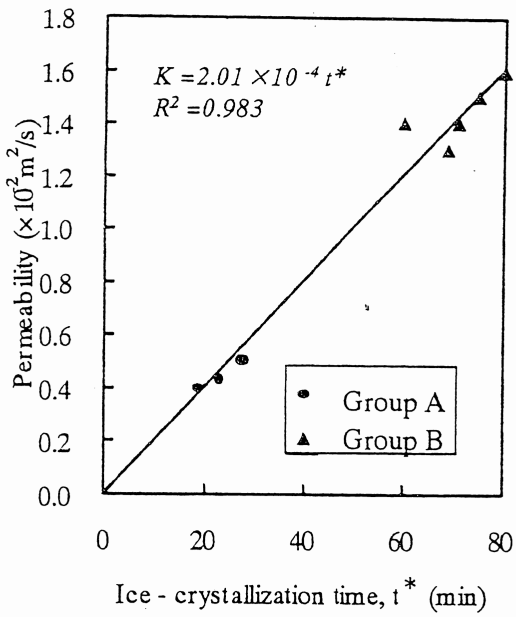


*Figure 9.* Permeability against ice-crystallization time.

the thermal conductivity of the dried layer as shown in FIGURE 6. In addition to concentration the permeability is influenced significantly by freezing manner, because the capillary-type ice columns is formed by ice crystals along with the direction of heat flow during freezing (Sagara, 1986), and the smaller size of ice crystals is formed with an increase in freezing rate. Consequently, the morphologies of capillary-type void as well as grain orientation and the pore size of the dried layer are arranged during a freezing process, and thus the transport properties of the dried layer are decisively governed by the structure fixed during freezing.

From these results, it would be suggested for liquid materials that under the constant solid concentration the material should be frozen in a manner to form straight ice columns whose orientation is parallel to that of heat transport during drying and also make larger ice crystals by employing the slower freezing rate. If the higher permeability coefficient could be obtained by controlling freezing method, the drying rate would be limited by heat transfer rate across the dried layer. Under this condition the surface temperature of the dried layer is allowed to increase within a certain range that is decided from the viewpoint of quality control for final products.

## NOTATION

$A$ = constant

$D_k$ = Knudsen diffusion coefficient, $m^2/s$

$d$ = diameter, m
$j$ = water-vapor flux, kg/(m$^2$-s)
$K$ = permeability, m$^2$/s
$k'$ = structural constant, -
$l$ = length, m
$\dot{m}$ = mass flux density, kg/(m$^2$-s)
$M$ = molecular weight, kg/mol
n = number of cells
$p$ = pressure, Pa
$\dot{q}$ = heat flux density, J/(m$^2$-s)
$R$ = gas constant, J/(mol-K)
$R_n$ = resistance against the water vapor, -
$R_s$ = equivalent resistance of each membrane, -
r = equivalent pore radius, m
$T$ = absolute temperature, K
$t$ = time, s
$\bar{v}$ = average molecular velocity, m/s
$X(t)$ = position of the sublimation front, -

*Greek letters*

$\delta_1$ = roughness factor of pore, -
$\varepsilon$ = porosity, -
$\theta$ = temperature, °C
$\kappa$ = Boltzmann constant
$\lambda$ = thermal conductivity, W/(m-K)
mean free path of the gas molecules, m in eqs. (3), (4), and (8)
$\sigma$ = diameter of a molecule, m
$\tau$ = tortuosity factor, -
$\Omega$ = total of separate contributions due to Poiseulle's flow, slip flow and Knudsen's flow, -

*Subscripts*

$c$ cell
$f$ sublimation front
$s$ surface
$w$ water vapor

## REFERENCES

1. Araki, T., Sagara, Y., Tambunan, A.H., and Kamaruddin, A., 1998, Measurement of Transport Properties for the Dried Layer of Several

Food Materials Undergoing Freeze-drying, Bul. Keteknikan Pertanian 12(2), pp.18-31

2. Harper, J. C., 1962, Transport Properties of Gases in Porous Media at Reduced Pressures with Reference to Freeze-Drying, AIChE J., 8(3) pp.298-302
3. Harper, J. C. and El Sahrigi, A. F., 1964, Thermal Conductivities of Gas-Filled Porous Solids, I & EC Fundamentals, 3(4), pp. 318-324
4. Bralsford, R., 1967, Freeze Drying of Beef, 1. Theoretical Freeze-Drying Rates of Beef, 2. A Calorimetric Method for Comparing Theoretical and Actual Drying Rates, J. Food Technology, 2, pp.339-353
5. Hoge, H. J. and Pilsworth Jr, M. N., 1973, Freeze Drying of Beef: Theory and Experiment, J. Food Science, 38, pp. 841-847
6. Triebes, T.A. and King, C. J., 1966, Factors Influencing the Rate of Heat Conduction in Freeze Drying, I&EC Process Design Development., 5(4), p.430-435
7. Ichiba, J., 1994, The Effect of Freezing Rate on Drying Characteristics of Granular Food Materials: Change in the Structure and Transport Properties, MD's Thesis, The University of Tokyo, pp.60-62
8. Kennard, E. H., 1938, Kinetic Theory of Gases, 149, McGrow-Hill
9. Mellor, J.D. and Lovett, D.A., 1964, Flow of Gases Through Channels with Reference to Porous Material, Vacuum, Vol.18, p.625
10. Mellor, J.D., 1978, Fundamentals of Freeze-Drying, Academic Press, London, pp.94-128
11. Sagara, Y., Kameoka, T. and Hosokawa, A., 1982, Measurement of Thermal Conductivity and Permeability of the Dried Layer during Freeze Drying of Beef, J. of Soci. Agr. Machinery, Japan 44(3)
12. Sagara, Y. and Hosokawa, A., 1982, Dry Layer Transport Properties and Freeze-Drying Characteristics of Coffee Solutions, Proc. Third Int. Drying Symposium (IDS'82), Birmingham, pp.487-496
13. Sagara, Y., 1986, Transport Properties Measurement of Food Sample Undergoing Sublimation Dehydration, Proc. Fifth Int. Drying Symposium (IDS '86), MIT, Cambridge, Vol.1, pp.413-421
14. Sagara, Y., 1992, Automatic Measurement System for Transport Properties of Food Samples Undergoing Sublimation Dehydration, Advances in Food Engineering, CRC Press, pp.111-124
15. Sagara, Y. and Ichiba, J., 1994, Measurement of Transport Properties for the Dried Layer of Coffee Solution Undergoing Freeze Drying, Drying Technology, 12(5), pp.1081-1103